$\bar{u}$ = superficial linear velocity of fluid phase, ft./sec.
$X$ = dimensionless group defined by Equation (3)
$Y$ = factor defined by Equation (18)
$Z$ = factor defined by Equation (20)

**Greek Letters**

$\alpha, \beta$ = constants in Equation (11)
$\delta$ = pressure drop per unit length calculated for single-phase flow, (lb.$_f$) (sq.ft.)/ft.
$\delta'$ = pressure drop per unit length calculated for two-phase flow, lb.$_f$(sq.ft.)/ft.
$\epsilon$ = void fraction of packed bed volume, dimensionless
$\theta$ = saturation factor, dimensionless
$\mu$ = fluid viscosity, lb.$_m$/(ft.) (sec.)
$\rho$ = fluid density, lb.$_m$/cu.ft.
$\phi$ = dimensionless groups defined by Equations (1) and (2)

**Subscripts**

$F$ = frictional pressure drop
$G$ = gas phase
$L$ = liquid phase
$LG$ = two phase
$T$ = total pressure drop

**LITERATURE CITED**


1. Dodds, W. S., L. F. Stutzman, B. J. Sollami, and R. J. McCarter, *AIChE J.*, **6**, 390 (1960).
2. Larkins, R. P., Ph.D. thesis, Univ. Michigan, Ann Arbor (1959).
3. Wen, C. Y., W. S. O'Brien, and L. T. Fan, *J. Chem. Eng. Data*, **8**, 47 (1963).
4. Lockhart, R. W., and R. C. Martinelli, *Chem. Eng. Progr.*, **45**, 39 (1949).
5. Larkins, R. P., R. R. White, and D. W. Jeffrey, *AIChE J.*, **7**, 231 (1961).
6. Ergun, Sabri, and A. A. Orning, *Ind. Eng. Chem.*, **41**, 1179 (1949).
7. Chisom, D., and A. D. K. Laird, *Trans. Am. Soc. Mech. Engrs.*, **80**, 276 (1958).



*Manuscript received November 17, 1965; revision received October 26, 1966; paper accepted October 28, 1966.*


# Transition and Film Boiling from Horizontal Strips


**R. C. KESSELRING, P. H. ROSCHE, and S. G. BANKOFF**

**Northwestern University, Evanston, Illinois**



**Measurements of heat flux and surface temperature fluctuations are reported for transition and film boiling of Freon 113 from flattened horizontal stainless steel tubes. The strip width is found to have a definite effect upon the heat flux in the film boiling regime. Photographic measurements indicate the absence of any appreciable long-range periodicities, from which it is inferred that random turbulent effects are quite important. Also, a spectrum of bubble diameters, frequencies, and spacings is observed. On the other hand, some short-time spatial periodicities were observed, and the theoretical values of the parameters fell well within the experimental range. Based upon the photographic and heat transfer measurements, a recommended expression for the minimum heat flux was developed.**


Unlike nucleate boiling, transition and film boiling of a pool of liquid from a horizontal heating surface may be independent of the nature of the heating surface, so that a purely hydrodynamic theory is possible. The basic theory is due to Zuber and Tribus (*1*), who assume that the frequency and spacing of vapor release points are governed by the stability of the interface between the vapor and the liquid. The spacing of vapor release points is determined by the wave number for Taylor instability of a liquid layer of semi-infinite extent lying over a lighter fluid which is also of semi-infinite extent. For the maximum heat flux in transition boiling, the maximum allowable relative velocity of the vapor jets leaving the surface and the liquid "spikes" returning to the surface is considered to be determined by Helmholtz instability of the respective interfaces. It is assumed that nowhere in the transition boiling region does the liquid come into contact with the heating surface.

The theory was subsequently modified by Zuber (*2, 3*), by Berenson (*4, 5*), and by Lienhard and Wong (*6*). Alternative models, based upon the assumption of liquid-solid contact in transition boiling, have also been proposed (*7*). Experimental measurements of bubble patterns and flux–$\Delta T$ curves have been made by Westwater et al. from tubes and flat plates (*8* to *10*) which support some aspects of the Zuber theory. A detailed review is given in reference *11*.


R. C. Kesselring is with North American Aviation, Canoga Park, California. P. H. Rosche is with M. W. Kellogg Company, Jersey City, New Jersey.


## EXPERIMENTAL EQUIPMENT

The boiling element consisted of a partially flattened ½ in. (O.D.) stainless steel tube 4.75 in. long (Figure 1). Flatness was checked visually by means of a straight edge. The tube was completely covered with ⅛ in. of epoxy resin with the exception of a heating strip surface. Nevertheless, a few bubbles were generated at minute pinholes in the epoxy, but were kept out of the field of view by deflector fins along each side of the heating surface. These fins also served to reduce flow toward the heating surface from the sides, which can frequently be troublesome in boiling from strips (*12*). Strip widths of both ½ and ¼ in. were used, the ¼-in. strip meeting the requirement of a single straight row of bubbles. To study the dependence of heat flux upon the width of the

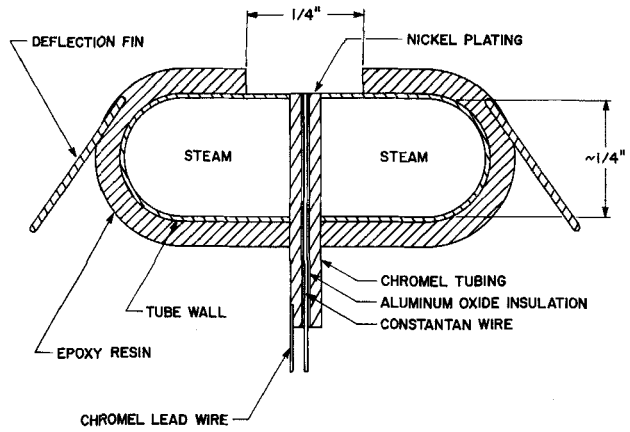


**Fig. 1. Experimental boiling element and detail of plated thermocouple construction.**

boiling strip, work was also done with ⅞-in. flattened tubes with strip widths of ¼, ½, and 1 in.

Freon 113 was boiled at atmospheric pressure in a cylindrical Pyrex section 8.8 in. in diameter and 6.0 in. in length, held between two ground steel end plates (Figure 2). The Pyrex glass was provided with a neck through which the boilup passed into a condenser. The boilup was led to a condenser by means of ⅝-in. copper tubing provided with external heating coils to ensure that no condensation occurred within the tubing itself.

Two commercial thin-film thermocouples, ($\tau \sim 1\mu$ sec.) were mounted in the stainless steel tube flush with the top of the surface. The assembly was then nickel-plated to 0.0001 in. thickness by vacuum deposition. Spot-welded 30- and 36-gauge surface thermocouples were also employed, but were thought to be less reliable than the flush-mounted thermocouples, which gave surface temperatures within 1° to 2°F. of computed values with the boiling cell empty. The thermocouple output emf was amplified and read out on a continuous strip recorder or a recording oscillograph.

High-speed photographs were taken with a Wollensak Fastax WF-3, 16-mm. camera at a final speed of 2,600 frames/sec. Timing marks were produced on the film by a neon timing light controlled by a Wollensak pulse generator. Lighting was provided by two 500-w. spotlights directed against a ground glass plate situated directly behind the cell.

## PROCEDURE

Prior to insertion in the boiling cell, the tube was given a surface finish with 2/0 emery cloth, followed with crocus cloth, until its appearance was clean and lustrous. The cell was then filled with Freon 113 to 2 in. above the surface of the tube and allowed to boil until the system reached steady state. Thermocouple output was then recorded and for photography runs the film was exposed at previously determined settings. To determine the heat flux at any point, the rate of boilup was obtained by measuring the time required to fill the calibrated glass section in the condensate return line. To account for vapor generated from other than the metal strip on the top surface of the flattened tube, the liquid level in the cell was decreased to just below the metal strip, and the boilup from this arrangement was similarly determined at the stream pressure inside the tube. The correction ranged from 8% at the peak heat flux to 57% at the maximum $\Delta T$ of 204°F.

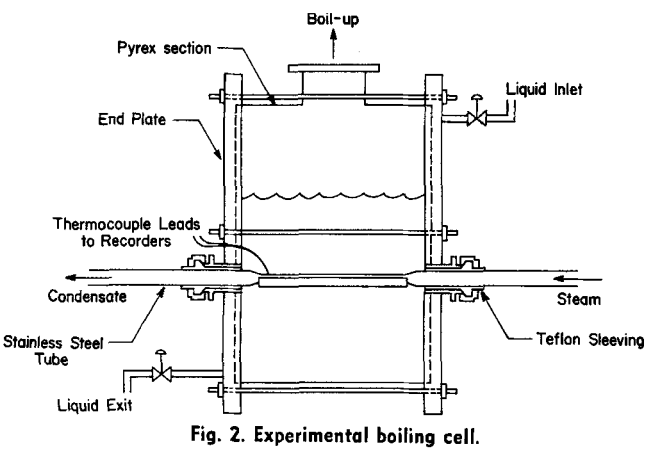


**Fig. 2. Experimental boiling cell.**

As a check on the heat flux, the amount of steam condensate emitted from the pressurized, insulated line was collected and measured. These heat balances closed within 15%. Since the latent heat of evaporation is much higher for water than for Freon 113, a much longer time was required to obtain a significant amount of condensate. Therefore, the boilup method was relied upon for most heat flux determinations, with the steam condensate method used occasionally as a check.

The heat input to the system was varied by controlling the inlet steam pressure. To avoid aging problems, the surface of the tube was refinished after each run.

The net vapor flow rate from the strip alone was obtained by taking the difference between the two boilup measurements mentioned above. The heat flux was then obtained from a knowledge of the dimensions of the strip and the heat of vaporization. To compensate for the nonuniform vapor temperature, vapor properties were evaluated at the mean temperature between saturation and the tube surface temperature. All strips employed were examined carefully to ensure that no cracks were present along the edges where the epoxy was applied. The scatter of data around the boiling curve was usually within ± 14%.

## RESULTS

### Effect of Strip Width

There was a definite dependency of the boiling curve (Figure 3) upon strip width. There seemed also, based upon visual impressions, to be some differences in the pattern of bubble release from the various width strips (Figure 4). To the naked eye the ¼-in. strip appeared to have a single row of bubbles, whereas two imperfect rows seemed to be present on the ½-in. strip. The bubble diameter at break-off was greater for the narrower strip. Similar observations were made by Westwater and Breen (*12*)

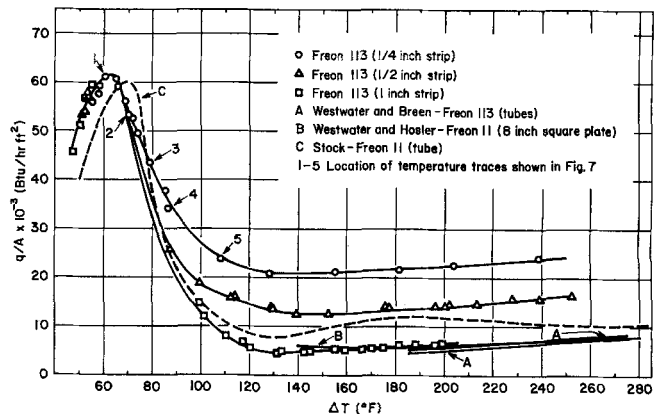


**Fig. 3. Comparison between boiling curves obtained for various strip widths.**

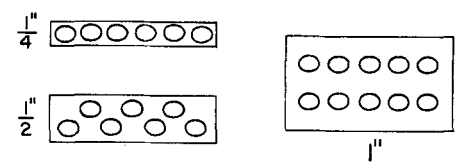


**Fig. 4. Visual observations of boiling on various width strips.**

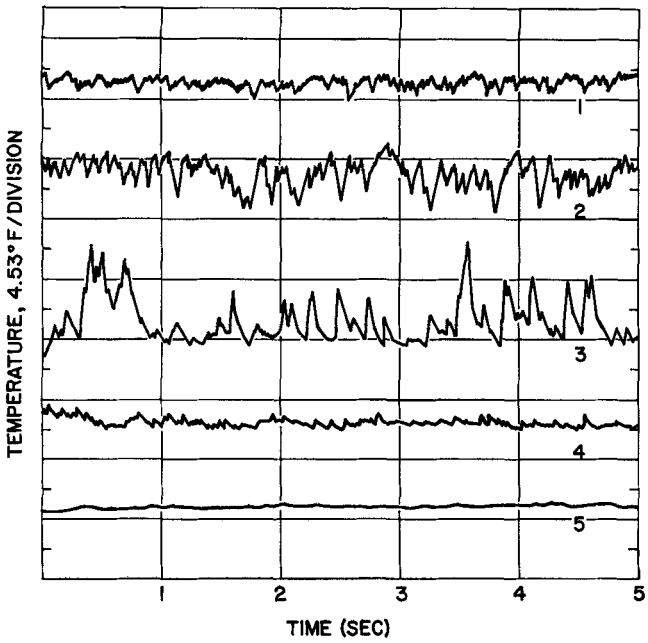


Fig. 5. Temperature traces of plated thermocouple during boiling from ¼-in. strip.

in boiling from horizontal cylinders. On the widest strip the active bubble centers at any instant formed a triangular lattice, characteristic of a two-dimensional disturbance for the Taylor theory, with a wavelength greater by a factor of $\sqrt{2}$ than in a single row of bubbles. This leads to a difference of a factor of 2 in the theoretical heat flux predictions. Similar differences appear in the Zuber and Berenson models (*1, 4*). It may be noted from Figure 3 that the Freon 113 boiling curve from the 1-in. strip is in good agreement with boiling curves obtained by various investigators (*9, 12, 14*) using Freon 113 as well as Freon 11.

Finally, it has been shown by Bernath (*19*) and Costello and Frea (*20*) that heater diameter influences pool boiling burn-out. The effect of flow from the sides, here minimized by the use of deflection fins, was also remarked by the latter investigators.

#### Surface Temperature Fluctuations

Traces of the temperature fluctuations for the plated thermocouple on the ¼-in. strip are shown in Figure 5. The location on the boiling curve corresponding to the various temperature traces is shown in Figure 3. The average of the five largest uninterrupted temperature deflections is seen to increase from about 3°F. at 18 cycles/sec. at the maximum flux in transition boiling to about 10°F. at 11 cycles/sec. midway in transition boiling. Surface temperature fluctuations then decrease again and stop entirely before the minimum flux in transition boiling is reached. No fluctuations were recorded in the film boiling region.

Traces of the temperature fluctuations recorded by the 36-gauge thermocouple spot-welded to the surface were also obtained. The average temperature fluctuation of this thermocouple also increased from about 5°F. at 18 cycles/sec. at the maximum flux in transition boiling to a value of about 25°F. at 16 cycles/sec. midway in transition boiling. Fluctuations from the 36-gauge couple, however, were observed to continue even in the film boiling region, where they appeared to maintain a steady amplitude of about 9°F. at 15 cycles/sec. Stock (*14*) recorded temperature fluctuations from 30-gauge thermocouples spot-welded on a tube and also noted that the fluctuations continued well into the film boiling region (by approximately 200°F.). It is believed that the continuance of fluctuations in the film boiling region, as measured with the 36-gauge thermocouples, is because the wires extending from the surface break up the thin vapor film, resulting in a temperature dip. To check this hypothesis, the flattened tube was rotated in the cell so that the exposed metal strip was facing downward. Boiling from this configuration results in a larger vapor film thickness and it was found that the temperature fluctuations of the 36-gauge thermocouple ceased to exist at moderate surface temperatures.

An effort was made to obtain a value for the thickness of the vapor film which might cover the surface in the region of transition boiling where surface temperature fluctuations were experimentally measured. The wall of the heated tube was assumed to be an infinite flat slab, initially at uniform temperature, whose surface temperature varied linearly with time. This problem has a standard solution (*15*) which permits the computation of the heat flux at the surface of the slab. This was then equated to the heat flux through the imagined vapor film. Based upon the slope of a typical dip in the measured temperature trace, the vapor film, if it existed, was estimated to have a thickness of the order of $10^{-5}$ cm., which is smaller than the characteristic surface roughnesses. Hence, for all practical purposes, solid-liquid contact definitely exists in the transition boiling regime.

#### Photographic Results

Six side-view films were taken of boiling on a ¼-in. strip, under conditions shown in Figure 6. Three films were also run, primarily for comparison purposes, viewing a ½-in. strip. To analyze the films, the length of the observed section of the tube, 5.34 cm., was then divided into ninety-six equal intervals, and the frequency and vapor volume for each interval were determined by tedious frame-by-frame measurements. For each bubble at the instant of break-off, the lengths of the major and minor axes were recorded. The bubble volume was estimated by assuming the bubble to be ellipsoidal in shape. The heat flux was then estimated from the total vapor volume computed for each film and the time required to run the film. As shown in Table 1 agreement between heat flux determined from condensate measurements and that estimated from the films was good.

To obtain quantitative information on the bubble release patterns, plots of bubble frequency and vapor volume vs. position along the strip were constructed. The plots shown in Figure 7, taken near the minimum heat flux, are, rather surprisingly, fairly characteristic of all the films from strips of both widths (*16*). In every film the vapor volume peaks roughly corresponded to the frequency peaks, although the location of these peaks shifted somewhat from film to film.

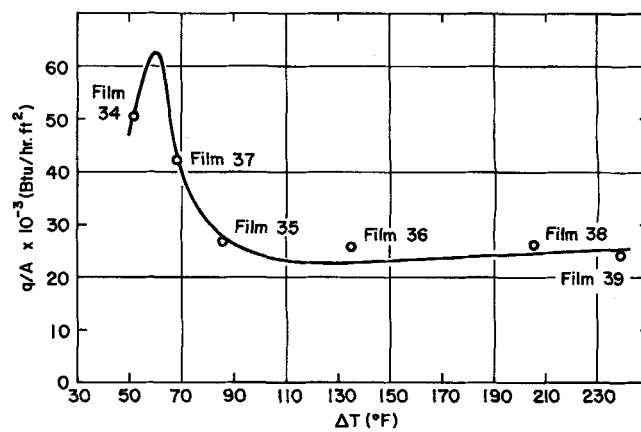


Fig. 6. Location of films taken of ¼-in. strip on boiling curve with Freon 113.

TABLE 1. PHOTOGRAPHIC MEASUREMENTS

¼-in. strip

| Film No. | $\Delta T$, °F. | Boiling regime* | Boil-up calc. lb./hr. | Boil-up exp., lb./hr. | Flux exp., (B.t.u./(hr.)(sq. ft.) | Bubbles/(sec.)(sq. cm.) | $D_e$, cm. | c-c† spacing, cm. | $\tau$,† sec. |
|---|---|---|---|---|---|---|---|---|---|
| 34 | 51.5 | N | 6.67 | 8.01 | 50,600 | 51.95 | 0.765 | 0.102 | 0.296 |
| 37 | 68 | T | 7.54 | 6.56 | 42,400 | 51.20 | 0.806 | 0.157 | 0.196 |
| 35 | 85.5 | T | 5.72 | 4.09 | 26,900 | 39.55 | 0.804 | 0.148 | 0.269 |
| 36 | 135 | $T_k$ | 5.73 | 3.71 | 25,900 | 38.60 | 0.827 | 0.172 | 0.236 |
| 38 | 205.5 | F | 5.24 | 3.48 | 26,100 | 35.50 | 0.842 | 0.172 | 0.258 |
| 39 | 239 | F | 3.64 | 3.08 | 23,950 | 30.40 | 0.786 | 0.133 | 0.390 |
| | | | | | ½-in. strip | | | | |
| 41 | 86 | T | 7.26 | 7.45 | 24,600 | 33.65 | 0.728 | 0.111 | 0.210 |
| 42 | 175 | $T_k$ | 5.42 | 3.90 | 14,200 | 33.00 | 0.686 | 0.116 | 0.206 |
| 43 | 252 | F | 5.10 | 4.14 | 16,300 | 32.20 | 0.692 | 0.107 | 0.228 |

* $N$, nucleate regime; $F$, film regime; $T$, transition regime; subscript $k$ indicates near minimum heat flux.
† Average values obtained by analyzing experimental data as reported; center-to-center spacing shown is $\lambda_m/2$.

In an effort to determine the dominant wave number, if any, a harmonic analysis of the data from each film was performed. Again the results turned out to be roughly similar, regardless of the strip width. As shown in Figure 8 no outstanding peak was observed within the expected wave number range or, for that matter, at any wave number. Nevertheless, the high sharp peaks observed in the plots of frequency vs. position are indicative of bubble release at preferred locations. Thus the harmonic analyses indicate that in the present system, bubble release in both transition *and* film boiling was not strictly periodic either in space or time. This contrasts with the periodic behavior which has been reported for film boiling from horizontal wires and tubes, which are, however, relatively streamlined bodies from the point of view of the circulation pattern induced by the boiling. One should note, on the other hand, that similar observations have not been made from flat horizontal plates. For this geometry, as in the present case (flat strips with deflection fins), flow around the bluff shape results in a highly turbulent wake. Thus, the high sharp peaks observed in the plots of frequency vs. position could be indicative of a quasiperiodicity in the bubble release pattern, subject to local random influences. Alternatively, edge and/or nucleation effects might also have resulted in preferred release points. It is not evident from the films which of these explanations might be correct. It is also important to note that, despite the absence of long-range order, approximately periodic short-range patterns frequently appeared. Similar structures were also observed in transition boiling from a flat plate (9).

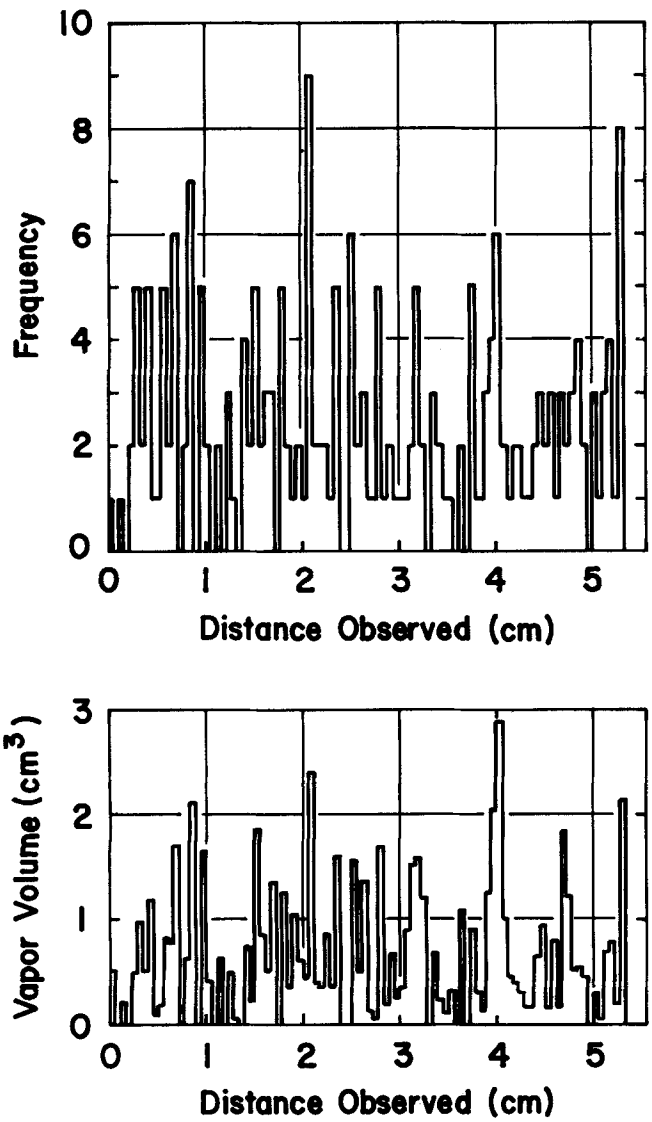


Fig. 7. Frequency of bubble release and vapor volume vs. distance from end of strip for film 36.

As noted above, a spectrum of release point spacings and bubble frequencies was observed. To determine the characteristic (or mean) wavelength and bubble frequency, it is convenient to define an activity distribution function $\eta(w)$ in the following way. Let $w$ be an integer in the range $(0, N)$, where $N$ is the largest number of bubbles observed leaving any interval in the observation time $t$, and $w_j \leq N$ be the value for the $j^{\text{th}}$ interval. Let $j \epsilon J$ imply that $w_j \geqq w$. Then $\eta(w) = \sum_{j \epsilon J} w_j / \sum_{j=1}^{96} w_j$ is the fraction of bubbles coming from sites with $w_j \geqq w$.

This procedure normalizes the bubble counts with respect to time and readily permits comparison of the different films. It is easily seen that as the bubble count $w$ increases, the activity $\eta$ decreases.

The average wavelength over the interval of tube observed can also be related to $w$. Since the postulated pattern of bubble release is an oscillating one with successive rows of bubbles displaced by half a wavelength, rather than a stationary standing wave, the average wavelength corresponding to a particular $w$ is given by

$$\lambda_w = \frac{2l}{X-1} \qquad (1)$$

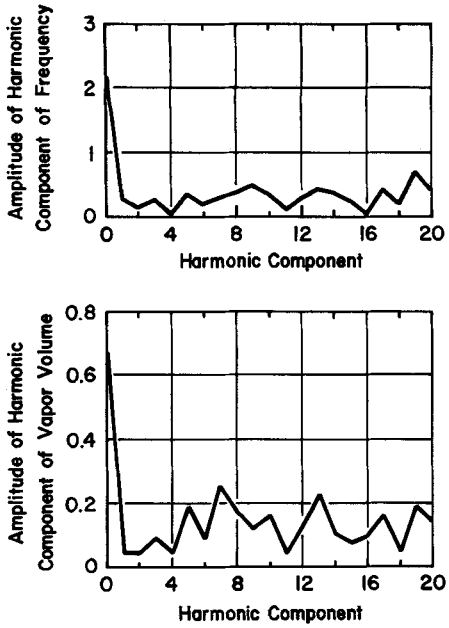


Fig. 8. Harmonic analysis for film 36.

where $X$ is the number of discrete values of $j \epsilon J$.

This assumes that such observed sites bound both sides of the observed length of tube. If this is not the case, $\lambda_w$ calculated can be in error by at most $4l/(X^2 - 1)$. This error is small for the smaller frequencies, while the high-frequency end of the curve of $\eta$ vs. $\lambda_w$ is very flat, so that negligible error results.

An average count $w_m$ for the ninety-six measurement intervals is given by

$$w_m = \frac{1}{96} \sum_{j=1}^{96} w_j.$$

This then yields a corresponding $\lambda_m$ from Equation (1). From this value the average frequency for sites spaced at $\lambda_m/2$ intervals is calculated from

$$\omega_{av} = \frac{\lambda_m}{2lt} \sum_{j=1}^{96} w_j \qquad (2)$$

With this procedure, plots were constructed of activity vs. wavelength for each film. All these graphs have the same general appearance. In fact, when all the data from the various films are presented on one graph, they fall on a relatively smooth curve, Figure 10, despite the fact that the regimes range from nucleate to film boiling. This seems to indicate that the distribution function of the bubble frequency remains approximately the same, regardless of the position on the boiling curve. If the phenomenon were strictly periodic, the plot of activity vs. wavelength would be a vertical line at some value of wavelength between $\lambda_c$ and $\lambda_D$.

According to the Zuber theory, the frequency and the heat flux should be almost directly proportional within the transition region, as the bubble break-off size and other hydrodynamic factors are considered to remain constant and the difference in sensible heat content would be small. As seen from Table 1, for a given width strip, the bubble break-off diameter is practically constant within the transition region, and is relatively invariant throughout all the regimes of boiling that were experimentally traversed. If the calculated values of heat flux and average frequency within the transition are used, the agreement is adequate, considering the uncertainties involved.

## COMPARISON WITH PREVIOUS STUDIES

The basic equation used by both Berenson and Zuber to describe the minimum heat flux may be written as

$$(q/A)_{\min} = \frac{L\rho_V \phi}{\tau} \qquad (3)$$

where $\phi$, the vapor volume per unit area per unit time, can be calculated by a variety of means, some entirely analytical and some partially experimental. A tabular comparison between the theoretical relations of Zuber and Berenson for the calculation of the minimum heat flux is shown in Table 2. The bubble pattern results are summarized in Table 3. From a comparison of the physical properties of Freon 113 and Freon 11, it appears that only small differences (3%) should occur in the theoretical results obtained with these two fluids used (*13*).

As noted above, the pattern of bubble release was not periodic, so that there was no unique bubble period. To compute an average value to compare with that of Westwater and Hosler, the average spacing reported by these investigators was taken as $\lambda_m$. From Figure 9 it was then determined what fraction of the bubbles came from centers having spacing of $\lambda_m/2$. The average frequency of bubble release from these centers was then calculated from

$$\omega_m = \frac{\lambda_m \eta}{2lt} \sum_{j=1}^{96} \omega_j$$

where $\tau_m = 1/\omega_m$, as given in Table 3. It is seen that there is reasonably good agreement.

It is also seen that the equivalent bubble diameter at break-off is relatively constant, but smaller than that reported by Westwater from top-view measurements at the estimated break-off time. It is thought that the present measurements are generally more reliable, since the break-off time is difficult to estimate from a top view. Bubbles continue to grow after detachment, and they generally assume a flattened shape as they rise.

As stated above, the 1-in. strip width permits a fully developed two-dimensional pattern of release points, simi-

TABLE 2. COMPARISON BETWEEN THEORETICAL METHODS OF ZUBER AND BERENSON FOR CALCULATION OF MINIMUM FLUX

| Method* | $\psi$ | $\phi$ | $D_b$ | $\tau$ |
|---|---|---|---|---|
| Zuber 1 | $2/\lambda_c^2 \tau$ | $\frac{\pi\lambda_c}{24}$ | $0.5\lambda_c$ | $6.3\alpha_1\beta$ |
| Zuber 2 | $2/\lambda_D^2 \tau$ | $\frac{\pi\lambda_D}{24}$ | $0.5\lambda_D$ | $14.3\alpha_1\beta$ |
| Zuber 3 | $2/\lambda_c^2 \tau$ | $\frac{\pi\lambda_c}{24}$ | $0.5\lambda_c$ | $7.5\alpha_2\beta$ |
| Zuber 4 | $2/\lambda_D^2 \tau$ | $\frac{\pi\lambda_D}{24}$ | $0.5\lambda_D$ | $9.9\alpha_2\beta$ |
| Zuber 5 | $2/\lambda_D^2 \tau$ | $\frac{\pi\lambda_D}{24}$ | $0.5\lambda_D$ | $8.1\alpha_1\beta$ |
| Berenson | $4/\lambda_D^2 \tau$ | $\frac{\pi\lambda_D}{18.6}$ | $0.432\lambda_D$ | $19.9\alpha_1\beta$ |

* Derivations are summarized in reference (*11*).

$$\alpha_1 = \left(\frac{\rho_L + \rho_V}{g(\rho_L - \rho_V)}\right)^{1/2}; \quad \alpha_2 = \left(\frac{\rho_L}{g(\rho_L - \rho_V)}\right)^{1/2};$$

$$\beta = \left(\frac{g_c\sigma}{g(\rho_L - \rho_V)}\right)^{1/4}$$

TABLE 3. COMPARISON OF EXPERIMENTAL PHOTOGRAPHIC RESULTS TO EXPERIMENTAL WORK OF OTHERS AND TO THEORY

| This work (Freon 113) | | | | | Westwater and Hosler (Freon 11 near minimum point) | | | Predicted values (Freon 113 at minimum point) |
|---|---|---|---|---|---|---|---|---|
| Strip width, in. | Boiling regime* | $\Delta T$, °F. | $D_e$ | $\tau_m$, sec.† | $D_e$, cm. | $\lambda_m$, cm. | $\tau_m$, sec. | Break-off diameter |
| ¼ | N | 51.5 | 0.765 | | 0.965 | 1.45 | 0.17 | Zuber |
| \| | T | 68.0 | 0.806 | | | | | $0.5\lambda_c = 0.356$ cm. |
| \| | T | 85.5 | 0.804 | | | | | $0.5\lambda_d = 0.617$ cm. |
| \| | $T_k$ | 135.0 | 0.827 | 0.210 | | | | Berenson |
| \| | F | 205.5 | 0.842 | | | | | $0.432\lambda_d = 0.533$ cm. |
| \| | F | 239.0 | 0.786 | | | | | Center-to-center spacing |
| ½ | T | 86.0 | 0.728 | | | | | $\lambda_c = 0.713$ cm. |
| \| | $T_k$ | 175.0 | 0.686 | 0.163 | | | | $\lambda_d = 1.233$ cm. |
| \| | F | 252.0 | 0.692 | | | | | Bubble period |
| Center-to-center spacing ($\lambda_m$) ~ 1.3 cm.‡ | | | | | | | | Zuber |
| | | | | | | | | $\tau_1 = 0.0678$ sec. |
| | | | | | | | | $\tau_2 = 0.154$ sec. |
| | | | | | | | | $\tau_3 = 0.0812$ sec. |
| | | | | | | | | $\tau_4 = 0.107$ sec. |
| | | | | | | | | $\tau_5 = 0.0870$ sec. |
| | | | | | | | | Berenson |
| | | | | | | | | $\tau = 0.215$ sec. |

* *N*, nucleate regime; *T*, transition regime; subscript *k* indicates near minimum point; *F*, film regime.
† Calculated by assuming $\lambda_m = 1.45$.
‡ Rough estimate based upon observations with the naked eye.

lar to that which might exist in film boiling from a flat plate. In fact, film boiling fluxes measured by Westwater and Hosler on an 8-in. by 8-in. surface agree very closely with those obtained in this work with the 1-in. strip. Upon taking into account the observed bubble patterns, a recommended expression for the minimum heat flux can be manufactured by the following reasoning. Using the experimental value of the minimum heat flux observed for the 1-in. strip, one can calculate the volumetric vapor flux at the minimum point. One would like now to find a combination of theoretical relations for the volumetric flux $\tau$ and $D_e$ that will be consistent with the measured overall heat flux and also with the photographic measurements made on the ¼- and ½-in. strips.

Since one row of bubbles appeared on the ¼-in. strip and two rows on the 1-in. strip, one concludes that the unconstrained bubble spacing ($\lambda_m$) is more closely approximated by the most dangerous wavelength (1.27 cm.) than by the critical wavelength. Similar views have been previously expressed (*4, 9*). It can be shown, moreover, that the form of a two-dimensional wave implies that four bubbles will appear per unit cell per period. It also appears reasonable that the diameter of the bubble at break-off from the 1-in. strip should be somewhat less than the value noted for the ½- and ¼-in. strips, since the total heat transfer is about the same. Referring to Table 3, a bubble diameter of either $0.5\lambda_d$ (Zuber) or $0.432\lambda_d$ (Berenson) seems likely. Berenson's experimental value was here chosen. Calculation of the mean bubble period as described above, which yields a result close to that of Westwater and Hosler, gives a value of approximately 0.17 sec. The $\tau_2$ expression due to Zuber (Table 2) is in good agreement with this figure. Using these expressions, we found that the value of the volumetric vapor flux was quite close to the experimentally observed value for the 1-in. strip. The recommended expression for the minimum heat flux is thus

$$(q/A)_{\min} = L\rho_V \frac{\pi}{6} D_b^3 \frac{4}{\lambda_d^2 \tau}$$

$$= 0.0806\, L\rho_V \frac{2\pi}{3^{5/4}} \frac{g_c \sigma g(\rho_L - \rho_V)}{(\rho_L + \rho_V)^2} \qquad (4)$$

It is important to note that if Zuber's, rather than Berenson's expression for the bubble diameter were substituted into Equation (4) for the minimum flux, the value would increase from 4,750 to 7,350 B.t.u./(hr.)(sq.ft.) for Freon 113. Thus, a 15% increase in the bubble diameter results in a 55% increase in the predicted minimum heat flux. By the same token a 55% error in the value of the bubble period would compensate for a 15% error in the bubble diameter (if both errors were in the same direction), and result in a correct prediction of the minimum heat flux. The strong possibility of compensating errors is one reason why experimental verification of analytical expressions for the minimum heat flux is so difficult. Nevertheless, considering that these heat balances are computed entirely from bubble number and bubble size measurements over a period of time, we see that the agreement is excellent.

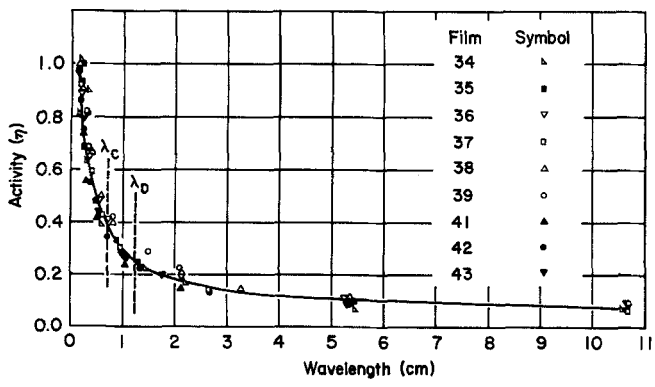


Fig. 9. Activity vs. wavelength: summary of test results.

## CONCLUSIONS

1. The geometric pattern of bubble release is an oscillating one, although not strictly periodic.
2. Contact between the solid surface and the liquid occurs during a portion of the transition boiling region but

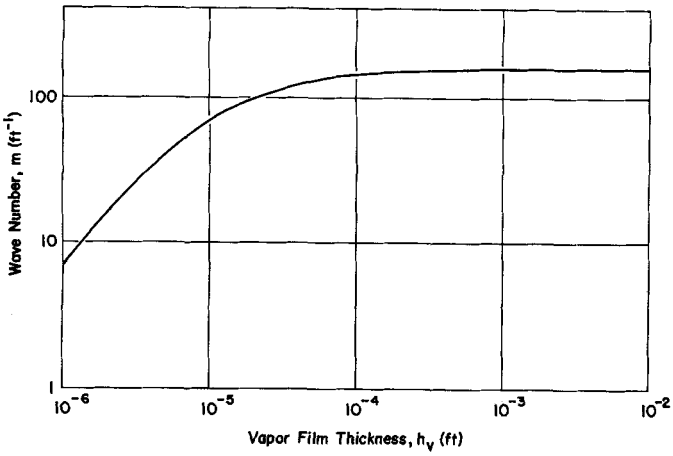


Fig. 10. Plot of wave number vs. vapor film thickness.

stops before the minimum point is reached.

3. The use of small horizontal strip widths results in restricted bubble patterns and consequently the minimum heat flux is found to be a function of strip width for small widths.

4. Strip widths in excess of $2\lambda_d$ should be used to obtain bubble patterns similar to those obtained on much larger surface areas.

5. A recommended expression for the minimum heat flux employs Berenson's value for the number of bubbles per area per time, Berenson's bubble diameter, and a particular relation of Zuber for the bubble period.

## NOTATION

$A$ = surface area, sq.ft.
$D_b$ = bubble diameter, ft.
$D_e$ = equivalent diameter, ft.
$g$ = acceleration of gravity, ft./sec.$^2$
$g_c$ = gravitational constant, 32.2 (lb.$_m$)(ft.)/(lb.$_f$)(sec.$^2$)
$h_L$ = height of liquid layer, ft.
$h_V$ = vapor film thickness, ft.
$l$ = length of tube under observation, ft.
$L$ = enthalpy change of vaporization plus sensible heat of vapor, B.t.u./lb.
$m$ = wave number, $2\pi/\lambda$, ft.$^{-1}$
$q$ = rate of heat flow, B.t.u./hr.
$t$ = time, hr.
$\Delta T$ = temperature difference between heated surface and boiling liquid at saturation, °F.

### Greek Letters

$\eta$ = activity, dimensionless, as defined above Equation (1)
$\lambda$ = wavelength, ft.
$\rho_L$ = density of liquid, lb.$_m$/cu.ft.
$\rho_V$ = density of vapor, lb.$_m$/cu.ft.
$\sigma$ = surface tension, lb.$_f$/ft.
$\tau$ = bubble period, sec.
$\phi$ = volume/(bubble)(area), ft.
$\omega$ = frequency of bubble release, sec.$^{-1}$

## LITERATURE CITED


1. Zuber, N., and Myron Tribus, *Rept. No. 58-5, U.C.L.A.*, Dept. Eng. (Jan., 1958).
2. Zuber, N., Ph.D. thesis, Univ. California, Los Angeles (June, 1959).
3. ———, *Trans. Am. Soc. Mech. Engrs.*, **80**, 711 (1958).
4. Berenson, P. J., *Tech. Rept. No. 17*, Massachusetts Inst. Technol., Cambridge (1960).
5. ———, *J. Heat Transfer*, **83**, 351-358 (1961).
6. Lienhard, J. H., and P. T. Y. Wong, *ibid.*, **86**, 224 (1964).
7. Bankoff, S. G., and V. S. Mehra, *Ind. Eng. Chem. Fundamentals Quart.*, **1**, 38-48 (1962).
8. Westwater, J. W., and J. G. Santangelo, *Ind. Eng. Chem.*, **47**, 1605 (1955).
9. Westwater, J. W., and E. R. Hosler, *A.R.S. J.*, **32**, 553 (1962).
10. Lienhard, J. H., and V. E. Schrock, *J. Heat Transfer*, **85**, 272 (1963).
11. Kesselring, R. C., Ph.D. thesis, Northwestern Univ., Evanston, Ill. (1966).
12. Westwater, J. W., and B. P. Breen, *Chem. Eng. Progr.*, **58**, 67-72 (1962).
13. E. I. du Pont de Nemours & Co., *Bull. B-2* (1957).
14. Stock, B. J., *Argonne Natl. Lab. Rept. No. 6175* (1960).
15. Carslaw, H. S., and J. C. Jaeger, "Conduction of Heat in Solids," 2 ed., Oxford Univ. Press, Oxford (1959).
16. Rosche, P. H., M.S. thesis, Northwestern Univ., Evanston, Ill. (1964).
17. Bankoff, S. G., *Phys. Fluids*, **2**, 576 (1959).
18. Bellman, R., and R. H. Pennington, *Quart. Appl. Math.*, **12**, 151 (1954).
19. Bernath, L., *Chem. Eng. Progr. Symp. Ser No. 30*, **56**, 95 (1959).
20. Costello, C. P., and W. J. Frea, *Chem. Eng. Progr. Symp. Ser. No. 57*, **61**, 258 (1965).


## APPENDIX: EFFECT OF VAPOR FILM THICKNESS ON MOST DANGEROUS WAVELENGTH

Bankoff (*17*) has shown that the wavelength which grows most rapidly in Taylor instability is given by*

$$[gm(\rho_L - \rho_V) - g_c\sigma m^3]\,[\rho_L h_L\, csch^2\,(mh_L) + \rho_V h_V\, csch^2\, mh] \quad (1A)$$

$$= [\rho_L \coth\,(mh_L) + \rho_V \coth\,(mh_V)]\,[g(\rho_L - \rho_V) - 3g_c\sigma m^2]$$

where viscous effects have been neglected. In many situations $mh_L >> 1$ and $mh_V << 1$, so that Equation (1A) becomes $g(\rho_L - \rho_V) - 3g_c\sigma m^2$

$$-\frac{[gm(\rho_L - \rho_V) - g_c\sigma m^3]\,[\rho_V h_V/(mh_V)^2]}{\rho_L + \rho_V/mh_V} = 0 \quad (2A)$$

which simplifies to the quadratic equation

$$\rho_L g\,(\rho_L - \rho_V) - \frac{2g_c\sigma m\rho_V}{h_V} - 3\rho_L g_c\sigma m^2 = 0 \quad (3A)$$

with the solution

$$mh_V = \frac{\rho_V}{3\rho_L}\left(-1 + \sqrt{1 + \frac{3g(\rho_L - \rho_V)}{g_c\sigma}\left(\frac{h_V\rho_L}{\rho_V}\right)^2}\right) \quad (4A)$$

It will be noted that for $mh_V \to \infty$, this gives the Bellman and Pennington (*18*) value for the most dangerous wavelength:

$$m = \sqrt{\frac{g(\rho_L - \rho_V)}{3g_c\sigma}} \quad (5A)$$

However, as $mh_V \to 0$, a Taylor series expansion gives

$$m = \frac{g(\rho_L - \rho_V)h_V}{2g_c\sigma}\,\frac{\rho_L}{\rho_V} \quad (6A)$$

In particular, as $h_V \to 0$, $m \to 0$, so that decreasing the vapor film thickness eventually has a stabilizing effect.

A plot of Equation (4A) for the Freon 113 system used in this work is shown in Figure 10. As noted by Berenson, the effect of vapor film thickness is negligible at $3 \times 10^{-4}$ ft. (or $10^{-2}$ cm.). This effect is therefore negligible in the present work, but may become important at very low pressures or at high surface temperatures.

* There is a misprint in Equation (6) of reference *17*.

*Manuscript received August 17, 1966; revision received October 31, 1966; paper accepted October 31, 1966.*